A Nature Portfolio journal



https://doi.org/10.1038/s43247-025-02465-0

Hydroclimate variability in the northern Caribbean during the last deglaciation was modulated by large-scale atmospheric circulation and climate events



Leah Travis-Taylor ® ¹ ⊠, Martín Medina-Elizalde ¹, Jesús M. Pajón ², Ambarish V. Karmalkar ® ³, Josué M. Polanco-Martínez ® ⁴, Christopher W. Kinsley ® ^{5,6} & David McGee ® ⁵

Marking the transition between the last glacial and Holocene, the last deglaciation featured rapid climate shifts including Heinrich event 1 and the Bølling–Allerød. This study presents the highest-resolution, continuous hydroclimate proxy records of this interval from the tropical Americas based on a precisely dated Cuban stalagmite. The records span 17.6–14.3 thousand years before present, revealing persistent interannual to multidecadal rainfall variability, attributed to El Niño-Southern Oscillation and Atlantic Multidecadal Variability. Broader centennial to millennial-scale trends are linked to major climate events. We observe peak aridity in western Cuba during Heinrich event 1.1 and 1.2 (~16.2 and ~15.1 thousand years before present), with preceding dry periods within chronological uncertainty, suggesting synchronicity. Wetter conditions and increased growth rates follow during the Bølling–Allerød. Model-based rainfall estimates support these results. Our proxy data highlight the dynamic nature of tropical hydroclimate, demonstrating wet and dry conditions fluctuate across timescales, despite climate state.

The last deglaciation, a pivotal period from approximately 19.0 to 11.7 thousand years (kyrs) before present (BP), represents a crucial phase in Earth's climate history marked by rapid and profound climate shifts between cold (stadial) and warm (interstadial) times that ultimately led to the Holocene. Significant climatic events during this period include Heinrich event 1 (H1) and the Bølling–Allerød (B/A) warm interval¹⁻³. Heinrich event 1 featured two phases of iceberg discharges impacting the Atlantic Meridional Overturning Circulation (AMOC)⁴. The phase with larger magnitude and impact, H1.1, peaked at 16.2 kyrs BP (15.5–17.1 kyrs BP) amidst cold North Atlantic conditions and a weakened AMOC, and coinciding with a rapid 2–4 °C warming in the subtropical eastern North Atlantic⁴⁻⁶. This phase was followed by the shorter and weaker H1.2 phase, peaking around 15.1 kyrs BP (14.3 to 15.9 kyrs BP), marked by minor North Atlantic cooling^{3,4,7}. Following H1, high-latitude northern hemisphere

climate warmed abruptly during the onset of the B/A period, spanning from 14.7 to 13.0 kyrs BP^{2,8}. These rapid climatic shifts were closely linked to AMOC and aligned with the interhemispheric thermal oceanic bipolar seesaw, where variations in the strength of AMOC led to opposite thermal responses in the Northern and Southern Hemispheres^{9,10}.

The last deglaciation was marked by significant hydroclimate changes across various low-latitude locations, linked as well via the ocean's bipolar seesaw. During H1, sediment reflectance records from the Cariaco Basin indicated drier conditions in northern Venezuela¹¹. Sediment cores from Lake Petén Itzá, Guatemala, revealed alternating clay and gypsum layers that reflect wet and dry climate conditions, respectively. These lithological changes are consistent with stable isotope ($\delta^{18}O$ and $\delta^{13}C$) records from the same archive, all of which indicate that the most arid periods coincided with Heinrich events $^{12-14}$. Conversely, a shift toward warmer and/or wetter

¹Department of Earth, Geographic, and Climate Sciences, UMass Amherst, Amherst, MA, USA. ²Department of Paleogeography and Paleobiology, National Museum of Natural History of Cuba, La Habana, Cuba. ³Department of Geosciences, University of Rhode Island, Kingston, RI, USA. ⁴Department of Statistics, Faculty of Sciences, University of Salamanca, Salamanca, Spain. ⁵Department of Earth, Atmospheric, and Planetary Sciences, MIT, Cambridge, MA, USA. ⁶Berkeley Geochronology Center, Berkeley, CA, USA. — mail: ltravistaylo@umass.edu

conditions in the Northern Hemisphere at the onset of the B/A is marked by declines in $\delta^{18}O$ and $\delta^{13}C$ and the cessation of in gypsum precipitation. During the B/A warm interval, low-latitude paleoclimate records across both hemispheres also indicate an out-of-phase hydroclimate pattern. These records suggest relatively wet conditions in the northern hemisphere, mirrored by drier conditions in the southern hemisphere^{2,8,15–18}, opposite to what is observed during H1.

This evidence of an out-of-phase tropical hydroclimate response has been generally interpreted as indicative of a mean latitudinal shift of the position the Intertropical Convergence Zone (ITCZ) and its belt of convective activity 17,19,20. However, recent paleoclimate reconstructions from the northern tropics, which lie beyond the direct influence of the ITCZ have revealed similar out-of-phase variability during the last glacial period²¹⁻²⁴, which suggests a more complex interplay of climate dynamics. Furthermore, modeling studies suggest that the ITCZ underwent only marginal shifts (likely less than 1° latitude) during past climate reorganizations, such as during the Last Glacial Maximum (LGM)^{25,26}. While precise bounds of ITCZ expansion and contraction during the deglaciation remain uncertain, some studies (e.g. 27,28) suggest that seasonal range variability in response to CO₂ changes may play a role rainfall shifts in the tropics. Regardless, these lines of evidence imply that changes in the ITCZ position alone likely do not account for observed broader tropical hydroclimate patterns, indicating a need for more comprehensive paleoclimate data and a deeper exploration of climate dynamics.

Stalagmites found in tropical and subtropical regions provide valuable archives for reconstructing past hydroclimate dynamics (Fig. 1). In particular, stalagmite $\delta^{18}O$ and $\delta^{13}C$ records offer critical insights into historical rainfall patterns. The $\delta^{18}O$ composition reflects the 'amount effect' in many tropical locations (Fig. 2)^{29–32} supporting inferences of past rainfall patterns, and even interpreted quantitatively in some studies^{23,31,33,34}. Additionally, stalagmite $\delta^{13}C$ represents another valuable proxy of rainfall variability.

Rainfall influences the extent of prior calcite precipitation (PCP), which is when degassing of the drip water occurs in air spaces prior to the site of stalagmite formation, causing calcite precipitation and impacting stalagmite δ^{13} C values³⁵. Notably, these proxies have been extensively analyzed in Caribbean regions like the Yucatan Peninsula, Belize, and Cuba, revealing significant aspects of past hydroclimate conditions^{22,28,36}.

Our new stalagmite OS stable isotope records represent the highestresolution, continuous speleothem paleoclimate record from Cuba during this interval, and are among the most detailed available for the tropical Americas, providing Northern Hemisphere insights that complement records from the Southern Hemisphere. OS, from Cuba's Majaguas-Cantera cave system, spans the time interval between 17.6 and 14.3 kyrs BP (Fig. 3), thus covering the last deglacial phase with high resolution (mean resolution: 3 ± 2 years). Our study presents detailed δ^{18} O and δ^{13} C records, offering fresh insights into hydroclimate variability during H1 and B/A intervals. Existing stalagmite records from Cuba mainly cover the last 12,500 years^{37–39}, with only one, Cuba Medio (CM), spanning the last deglaciation²². During the interval covered by our records, however, CM has a hiatus between 16.5 and 17 kyrs BP, in addition to much lower resolution of ~9 years (14.3-16.5 kyrs BP) and ~53 years (17-17.6 kyrs BP)²². Our new stalagmite OS stable isotope records not only offer the highest resolution, continuous speleothem paleoclimate study during this interval from Cuba to date, but also from the broader tropical Americas, across both hemispheres⁴⁰.

Considering this, the nature of our OS records allows observation of higher-frequency hydroclimate variability on interannual to multidecadal timescales. In particular, the role of large-scale climatic phenomenon such Atlantic Multidecadal Variability (AMV) and El Niño-Southern Oscillation (ENSO) in influencing circum-Caribbean hydroclimate can be examined. The AMV has been found to impact hydroclimate in the region through various means, such as by influencing convection and modulating the

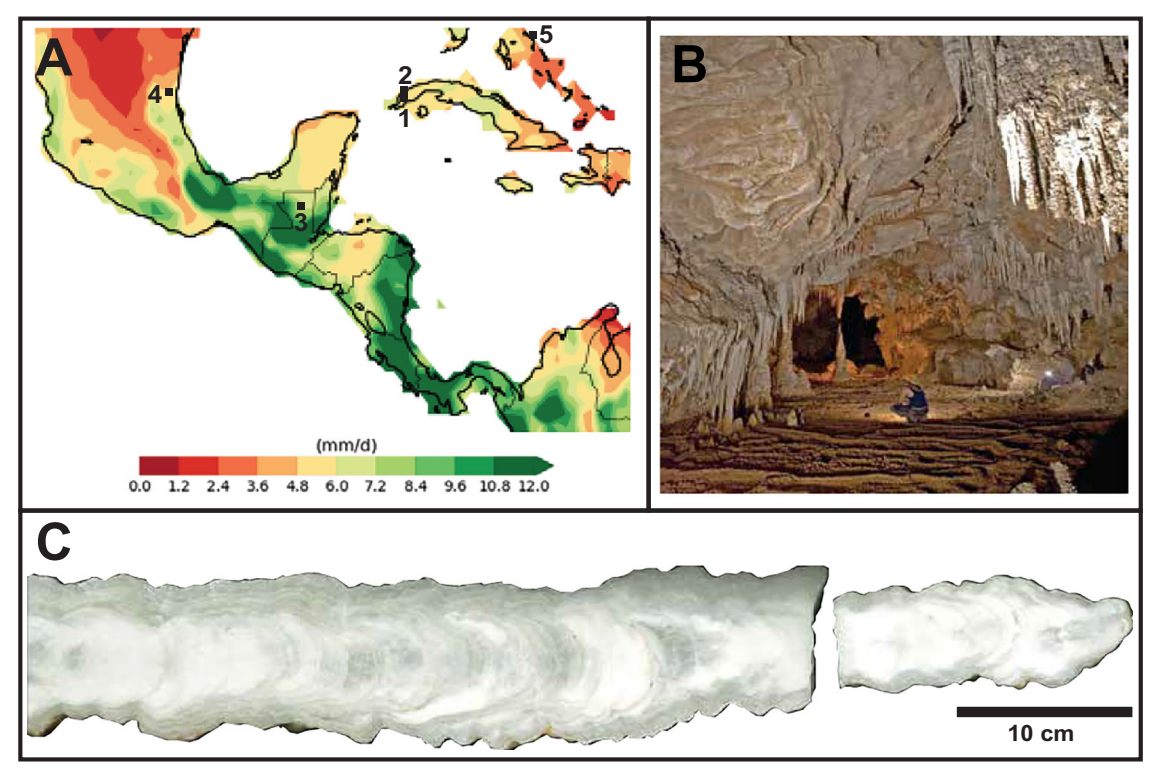


Fig. 1 | Cave location presented with marked regional studies and images of the Oliva (OS) specimen and collection site. A Map of Cuba and the surrounding Caribbean region showing the locations of OS collection site and surrounding referenced studies: (1) the Majaguas-Cantera cave system (MCCS; 22°23′N; 83°58′ W); (2) Santo Tomas Cave system, W. Cuba records (CM)²², (3) Lake Peten Itza,

Guatemala records^{12,13,91}; (4) Cueva Bonita, NE Mexico record (CB2)²¹; and (5) Abaco Island, Bahamas records^{51,68}; Shading represents rainy season (June-Oct) rainfall amount (mm/day) using the GPCC observational dataset (1981-2015)¹¹¹. **B** Picture of OS stalagmite collection area inside *Salón de la Permanencia Subterránea*, within MCCS. **C** The 640-mm-long OS stalagmite specimen.

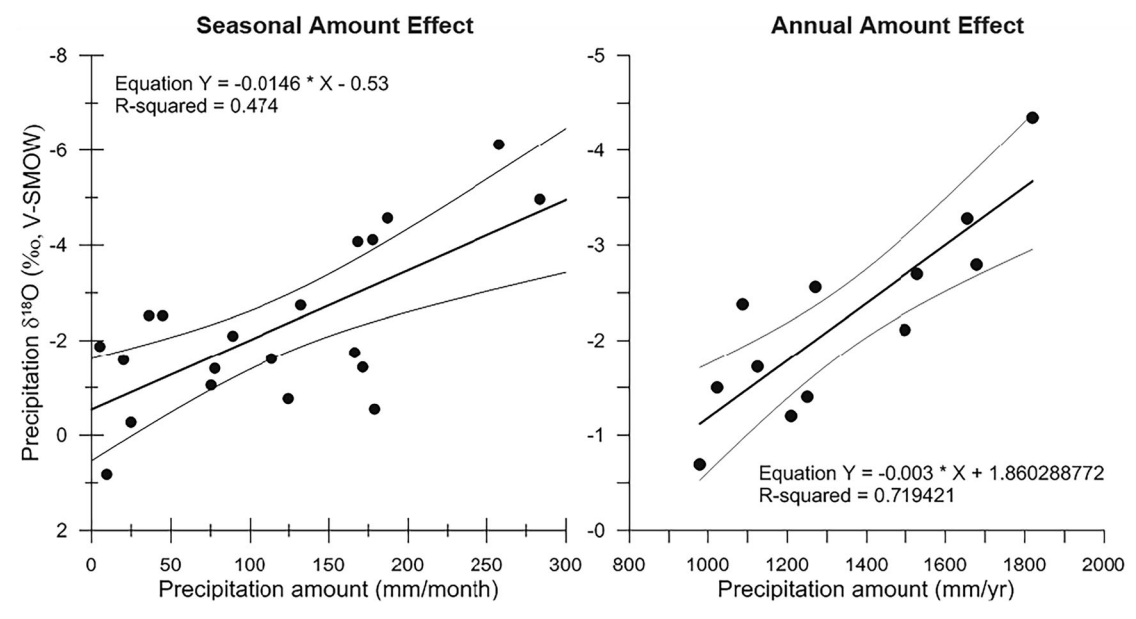


Fig. 2 | Plots of IAEA-GNIP rainfall data from Havana, Cuba. The amount effect is demonstrated locally on seasonal (left) and annual (right) timescales.

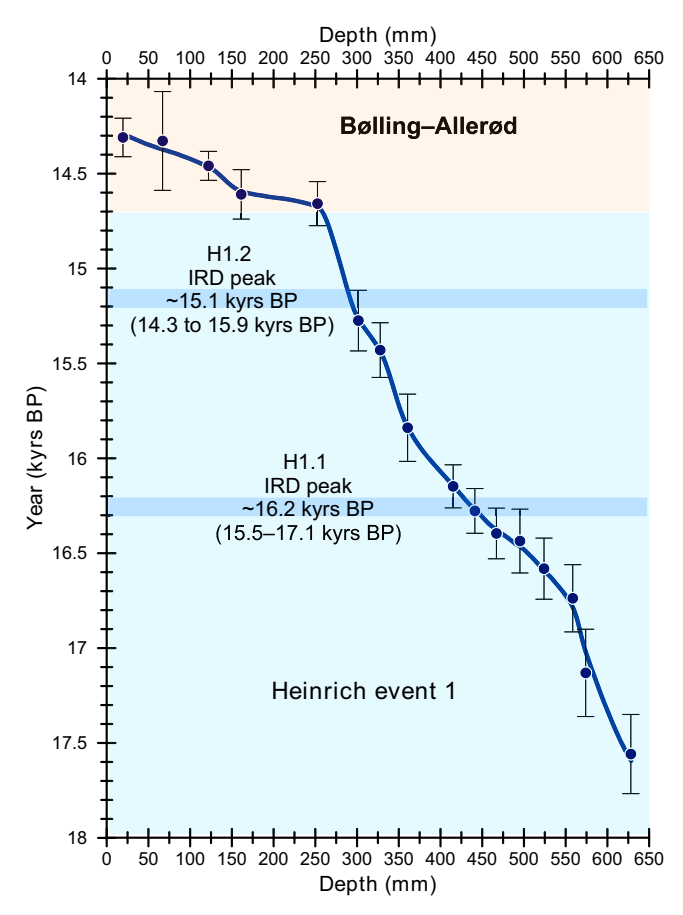


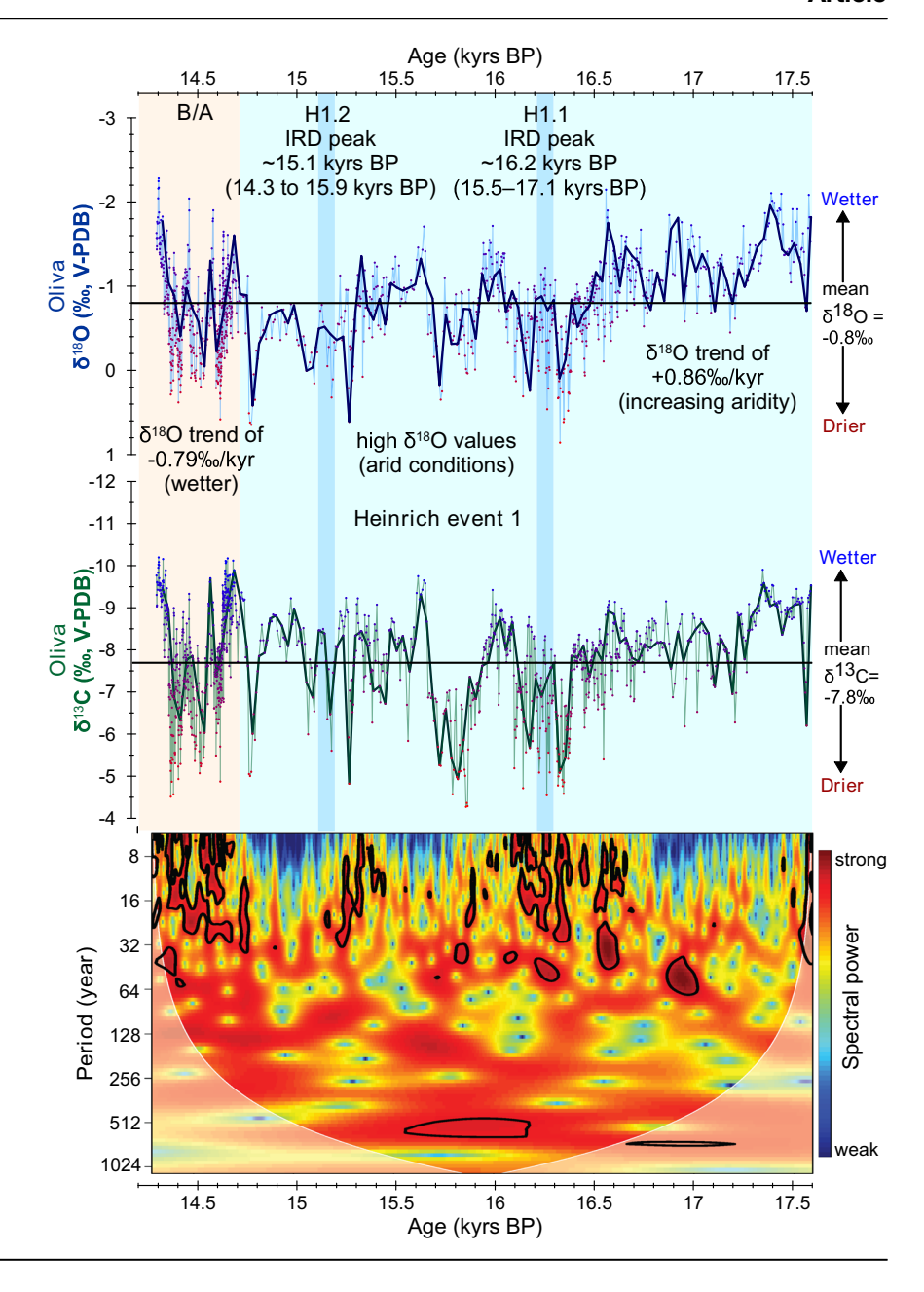
Fig. 3 | OS age versus depth with the 16 absolute U/Th ages and associated error bars (\pm 2 σ ; <1.4%). The OS chronology was created using COPRA (v. 1.16)⁸⁹ in MATLAB (v. R2021b). Blue and Orange shading represents timing of Heinrich Layer 1 stages (1.1 and 1.2) and the Bølling–Allerød (B/A) warm interval, respectively. Notice OS growth rate has a three-phase variability, with the fastest growth occurring during the last 400 yrs of the record (14.3–14.7 kyrs BP), the slowest growth between 14.7 and 16.1 kyrs BP, and relatively slow growth from 16.1 kyrs BP until the beginning of the record at 17.6 kyrs BP.

intensity of Atlantic tropical cyclones, which can affect regional rainfall patterns^{41–44}. ENSO also imprints periodicities into regional rainfall records by altering tropical cyclone frequency and intensity^{23,43,45,46}. OS records enable investigation of the results of these internal climate variations on rainfall patterns across multiple climate states.

Our study falls within the 'Mystery Interval' (MI; 17.5–14.5 kyrs BP) of the last deglaciation, a period characterized by a climatic paradox^{47,48}. According to hydroclimate records, there is a twofold division of the MI, with a global hydrologic reorganization occurring at ~16.1 kyrs BP^{47,49}. Lowlatitude hydroclimate records during this interval exhibit notable antiphase variability between the hemispheres, aligning with shifts in the tropical rainfall belt and suggesting profound changes in ocean circulation, in line with the bipolar seesaw mechanism and often with a hydroclimate shift in the mid-MI. However, indicators of ocean circulation, such as ²³¹Pa to ²³⁰Th ratio in Atlantic sediments⁵⁰ and the rate of ¹⁴C decline⁴⁸, imply that AMOC was significantly weakened during the entire interval, with no notable early to late MI transition in north Atlantic deep water production⁴⁷. This interplay between high-latitude climate shifts and tropical hydroclimate changes during H1 and the B/A sets the stage for understanding the complex dynamics of the MI. Opportunely spanning 17.6-14.3 kyrs BP, the OS records will allow examination of the hydroclimate changes from the northern Caribbean during the MI.

To contextualize our study within the broader regional narrative, it is essential to consider the diverse hydroclimate patterns revealed by paleorainfall records across the circum-Caribbean region during the last glacial and the MI. These records, encompassing areas such as the Gulf Coast of Mexico, Guatemala, Cariaco Basin, Bahamas, Cuba, and Puerto Rico, have indicated distinct trends and variability during these time intervals and particularly during the H1 to B/A transition $^{12,13,19,21,22,51}.$ For instance, the single speleothem $\delta^{18}\mathrm{O}$ record covering the last deglaciation in the northern Caribbean, albeit discontinuously, notably does not exhibit a distinctive transition between H1 and the B/A (CM record from Cuba²²). This contrasts with other tropical hydroclimate records that show a transition from dry H1 to wet B/A conditions, such as the sediment reflectance record from the Cariaco Basin¹⁹ and the speleothem stable isotope record from Northeast Mexico²¹, thus presenting an uncertainty in our understanding of these climatic phases. Our northern Caribbean stalagmite stable isotopic records cover this transition continuously with high resolution, allowing new insight into the deglacial interval.

Fig. 4 | Top panel: OS stalagmite oxygen (blue) and carbon (green) isotope records. Darker overlay lines are running averages with a resolution of 50 years. OS isotopic records cover the interval from 17.6 to 14.3 kyrs BP. Timing of Heinrich event 1 and distinct peaks in ice-rafted detritus (IRD) of Heinrich Layer 1 (from ref. 4), as well as the Bølling-Allerød (B/A) warm interval, are shown on the plot (blue and orange bars, respectively). Mean of both $\delta^{18}O$ and $\delta^{13}C$ records are denoted with a solid black line. Data symbols are red shaded if higher than the mean (drier), and blue shaded if lower than the mean (wetter). Lower panel: wavelet spectral power analyses of OS oxygen isotope record. Higher intensity of the color is indicating more power over a specific periodicity range within that same time interval. This indicates that periodicity range in particular (e.g., 8 years) is more strongly represented in the timeseries. The area outside the white curves indicates the cone of influence where the edge effects of the wavelet transform and uncertainties become important. Black contours reflect statistically significant power spectra (CI = 95%) (see Methods and Supplementary (page 6) for details).



This study allows detailed investigation into hydroclimate variability during the last deglaciation in the Northern Caribbean, focusing on: 1) the role of the ITCZ, SSTs, and other climatic factors in modulating rainfall patterns across interannual to millennial timescales, and; 2) comparing our findings with established records to explore the broader implications for regional climate history.

Results and discussion OS stalagmite growth rates

The OS stalagmite grew continuously from 17.6 to 14.3 kyrs BP, covering the last deglaciation time interval, including H1 and the B/A. OS's growth rate showed three distinct phases of variability. From 17.6 to 16.1 kyrs BP, stalagmite growth rates remained relatively low, averaging 0.2 mm/year. The slowest growth occurred between 16.1 and 14.7 kyrs BP, with an average rate of 0.1 mm/year, during H1.2. The fastest growth occurred in the latest 400 years of the record (from 14.7 to 14.3 kyrs BP) at an average rate of 0.9 mm/year, peaking at 4 mm/year approximately at 14.6 kyrs \pm 0.168 kyrs BP, coinciding with the onset of the B/A (Figs. 3, S1).

Oxygen and carbon isotope results

The reconstructed hydroclimate record is based on 1219 stalagmite stable isotope analyses, sampled at a 0.5 mm interval, providing a mean temporal resolution of 3 \pm 2 years (1 SD) (Figs. 4, S1). OS stalagmite calcite δ^{18} O values vary from 0.8% to -2.4%, while the δ^{13} C values range from -4.3% to -10.2% (Fig. 4). A statistically significant positive isotopic trend (p < 0.01) is observed in the OS δ^{18} O record with a slope of 0.86% per kyr from 17.6 to 16.3 kyrs BP, coinciding with a period of slow growth rates (<0.5 mm/year), as opposed to growth rates of nearly 4 mm/year later in the record (after ~15 kyrs BP). This can also be observed in the temporal resolution trends (Fig. S1). Between 16.3 and 14.7 kyrs BP, the δ^{18} O and δ^{13} C values show considerable oscillations, with positive isotopic values peaking at 14.7 kyrs BP, before the onset of the B/A. We note that the most negative isotopic excursions during the later interval from 16.3 and 14.7 do not reach levels that are as negative as those observed during the first 700 years of the record (Fig. 3). From 14.6 to 14.3 kyrs BP, a statistically significant negative trend (p < 0.01) emerges, with a slope of -0.79% per kyr, featuring a pronounced decline during the last century of the record, within the B/A (Fig. 3). Lastly,

the trends observed in the OS stalagmite δ^{18} O record are mimicked by the δ^{13} C record (Figs. 4, S2).

Wavelet spectral analysis

Wavelet spectral analysis results reveal significant variability in both the $\delta^{18}O$ and $\delta^{13}C$ records across interannual, decadal, and multidecadal timescales (Fig. 4). Plots of these results are interpreted by looking for clusters of strong spectral power spanning the same time interval. Our results indicate that the record has dominant periods as short as 8 years and as long as 128 years, with periods between these two extremes also suggested. Additional fluctuations occurring at approximately at ~6-year intervals are detected during high-resolution segments such as the window from 14.3 and 14.7 yrs BP, coeval with the B/A. These results are robust even when considering chronological uncertainties (detailed in the Supplementary Information; Fig. S4). These cyclicities may occur throughout the record, but we cannot identify them during the lower resolution intervals.

Interpretation of stalagmite OS proxies

Tropical speleothem δ^{18} O records are generally interpreted to reflect past rainfall variability, primarily via the existing inverse relationship between the amount of rainfall and its oxygen isotope composition (amount effect), which has been observed in the instrumental record (Fig. 1) and confirmed via model simulations³⁰. In this context, lower δ^{18} O values in the OS stalagmite are interpreted to correspond to lower δ^{18} O values in rainfall and, consequently, higher rainfall amounts^{22,37,39,52}. Within the MCCS, observational data indicate that stalagmite δ^{18} O effectively integrates variations in rainfall δ^{18} O, with the lowest δ^{18} O values aligning with periods of more substantial rainfall and increased drip rates⁵³. Notably, the impact of evaporation on the rainfall δ^{18} O signal appears to be negligible, as the signal is efficiently transmitted to drip sites³⁸. Moreover, the cave temperature within the MCCS remains remarkably stable throughout the year, with fluctuations typically confined to a range of \pm 0.2 °C. Importantly, this cave temperature is consistently over 3 °C cooler than the mean annual surface temperature^{37,52}

We propose that rainfall is the primary driver of carbon isotope variability in the MCCS as well, impacting processes like bedrock contributions, CO₂ degassing, soil moisture, and productivity. Stalagmite δ¹³C likely reflects rainfall changes, with elevated δ^{13} C during reduced rainfall. The strong correlation between OS δ^{13} C and δ^{18} O records (Figs. 3, S2) supports our interpretations. This correlation suggests that moisture source changes do not control past rainfall δ^{18} O variability, and that δ^{13} C records rainfall amount through rock-water interactions. Furthermore, while vegetation type can influence speleothem carbon isotopes³⁵, in low-latitude karstic environments, like the MCCS, the vegetation overhead remains relatively stable over time, and the soils tend to be shallow^{28,36,54}. These interpretations are consistent with previous stalagmite research conducted in western Cuba for this interval (e.g., lower P/Ca ratios in stalagmite CM during the last deglacial vs. the LGM)²², as well as in the Yucatán Peninsula³⁶, and particularly supported by concurrent variability of stalagmite stable isotopic and trace elemental compositions reflecting PCP³⁵.

As one additional hydroclimate proxy, we also plotted the $\delta^{234}U_{initial}$ values from our OS U-series dates (Table S2 and Fig. S8). The $\delta^{234}U_{initial}$ of speleothems indicates the $^{234}U/^{238}U$ disequilibrium of the formation water 55 . Related to weathering and water-rock interactions, higher $\delta^{234}U_{initial}$ values have been found to correspond to drier conditions due to weaker weathering and longer residence times of water in the karst, while lower values point to wetter intervals due to increased infiltration times and bedrock dissolution 55,56 . For example, a recent study interpreted $\delta^{234}U_{initial}$ as a hydroclimate proxy and found a relationship between $\delta^{234}U_{initial}$ and their $\delta^{13}C$ and Mg/Ca records 56 .

Interdecadal to multidecadal hydroclimate variability

The available evidence, including instrumental data, paleoclimate records, and modeling studies, points to a significant connection between the Atlantic Multidecadal Variability (AMV), which is the internal variability of

SSTs in the North Atlantic on multidecadal timescales, and hydroclimate patterns in the Caribbean and Gulf of Mexico regions^{37,42,57-60}. Studies have consistently shown a positive correlation between the AMV and rainfall, particularly in western Cuba (i.e., higher SSTs correlated to more rainfall)^{37,38,61}. Additionally, the strong decadal climate signal observed in the modern Northern Caribbean has been attributed to AMV-related influences⁶².

We propose that the OS stalagmite's stable isotope records, reflecting decadal to multidecadal rainfall variations, are likely connected with the dominant North Atlantic SST variability pattern associated with the AMV. This AMV-driven hydroclimate response in the Atlantic Basin is thought to be associated with changes in convective activity related to the ITCZ and an enhanced SST gradient across the equator⁴¹. The AMV has also been found to impact the intensity of Atlantic tropical cyclones, which can further affect regional rainfall patterns in the northern Caribbean region along their path⁴¹⁻⁴⁴. While this study focuses on hydroclimate variability during the last deglaciation, the role of AMV in modulating hurricane frequency and intensity remains an important avenue for new research. Although further work is needed, future analyses could examine the co-variability of δ^{13} C and δ¹⁸O as potential indicators of tropical cyclone-related rainfall, given their shared sensitivity to intense precipitation events. Additionally, a more comprehensive analysis incorporating additional speleothem records alongside sedimentary archives from mangrove cores, Gulf of Mexico deposits, and the Mississippi Fan could provide valuable insights into longterm hurricane variability in response to past climate shifts.

Furthermore, the higher frequency variability observed at approximately 6-year periods is likely influenced by the El Niño-Southern Oscillation (ENSO) and its modulation of Caribbean hydroclimate. Studies have demonstrated that variations in Atlantic tropical cyclone activity impact rain amounts in the northern Caribbean on interannual to interdecadal timescales. ENSO likely plays a crucial role in imprinting these periodicities into regional rainfall records by modulating tropical cyclone frequency and intensity^{23,43,45,46}. During El Niño conditions, ENSO leads to decreased hurricane activity due to increased wind shear in the Atlantic⁶³⁻⁶⁵ and therefore rainfall contribution from tropical waves and cyclones are expected to decline in their regions of influence⁴³. Importantly, these dominant variability periods revealed by the OS stalagmite records are consistently observed across the Caribbean region, highlighting the significant roles of both AMV and ENSO throughout various climatic periods, including the Holocene, the deglaciation, and the last glacial period e.g refs. 23,24,37,66'.

Comparison with local and regional records

Comparing the $\delta^{18}O$ records of the OS stalagmite from the MCCS and the CM stalagmite from Santo Tomas cave in Cuba (25 km away) reveals significant differences in both absolute values and isotopic amplitude. The OS stalagmite displays more than twice the $\delta^{18}O$ amplitude of the CM stalagmite ²² (Fig. 5). The particularly high average $\delta^{18}O$ values in the CM record at this time (0.8 to -0.9% range; 0.1% average) as opposed to the $\delta^{18}O$ value ranges CM recorded at different times (e.g., 1 to -4% range over the entire record of 7 to 96 kyrs BP), and versus those in OS (0.8 to -2.4% range; -0.8% average), suggest that evaporative processes may have influenced the CM record during this specific interval. Empirical isotopic equilibrium calculations suggest that stalagmites precipitating near equilibrium should show $\delta^{18}O$ values between -2.9 to 0.5% one of the CM record with OS.

Although comparisons are limited by resolution issues between 15.0 to 17.0 kyrs BP and geographical differences, the OS δ^{18} O record is consistent with the AB-DC-09 speleothem record from the Bahamas, which has a similar drying trend near the early part of the record (~17.5 to 17 kyrs BP). Arid conditions and low growth rates continued until ~15 kyrs BP in both records, when a shift to lower δ^{18} O values (wetter conditions) started (Fig. 6E)^{51,68}. While only available from the beginning of our record until ~15.5 kyrs BP, the Puerto Rican speleothem (PR-LA-1)²⁴ has a drying trend from ~17.5 through 15.5 kyrs BP, comparable to the OS trend, and contains three positive δ^{18} O excursions (peaks of aridity) of at least 1‰, all of which

17.5

are associated with a similar interval in the OS δ^{18} O record (Fig. 6D). Additionally, we find a speleothem from NE Mexico, CB2, records a drying trend from the beginning of our record until ~16.8 kyrs BP, and then a gradual to sharp shift to wetter conditions around ~14.8 kyrs BP (Fig. 6F)²¹. This longer-distance connection to the northern Caribbean is potentially linked to the CLLJ extending over both Cuba and Mexico²¹.

Hydroclimate variability during H1

To ensure clarity and consistency, we adopt the definitions of Heinrich events as outlined in ref. 4 and related sources. A Heinrich event refers to a period of abrupt climate change suggested to be driven by the massive discharge of icebergs from the Laurentide Ice Sheet into the North Atlantic. The Heinrich layer is the distinct sedimentary deposit in marine sediment cores that serves as physical evidence of these events. A Heinrich stadial is a broader cold climatic period during which a Heinrich event occurs; however, not all stadials contain Heinrich events.

Previous studies have identified two phases within Heinrich event 1 (H1). The larger phase, H1.1, peaked at $\sim\!16.2$ kyrs BP (15.5–17.1 kyrs BP) during cold North Atlantic conditions and a weakened AMOC. This period coincided with a 2–4 °C warming in the subtropical eastern North Atlantic^{4–6}. The shorter and weaker H1.2 phase peaked around $\sim\!15.1$ kyrs BP (14.3–15.9 kyrs BP) and was marked by minor cooling^{3,4,7}. During H1, especially in its latter phase, the AMOC weakened significantly, impacting hydroclimate patterns as shown by various tropical hydrological records documenting substages across the equator 13,15,17,19,69 .

Data from OS demonstrate a two-step pattern during H1: a first period from 17.6 to 16.1 kyrs BP, followed by a period from 16.1 to 14.7 kyrs BP. This pattern is evident in both growth rate variations (Figs. 3, S1) and in the average δ^{18} O and δ^{13} C values (Fig. 4), as well as the δ^{234} U_{initial} values (Fig. S8). The δ^{18} O record of the OS stalagmite suggests peak aridity in western Cuba coinciding with both the peaks of H1.1 at 16.2 kyrs BP and H1.2 at 15.1 kyrs BP. These periods of peak aridity, indicated by the highest δ^{18} O values, align with the weakest phases of the AMOC. The positive shifts in our OS δ^{18} O record also match very closely (considering chronological error) with abrupt monsoon weakening recorded in two speleothem hydroclimate records from Hulu Cave, China (YT and PD; Fig. S7) around the peak of H1.115,49. During the early phase of H1, we find more humid conditions with lower OS stalagmite δ^{18} O values before 16.4 kyrs BP. The dual-phase pattern in the OS δ¹⁸O record thus closely aligns with the updated timeline for H1⁴, and notably, with the two peaks of aridity in western Cuba. Given terrestrial amplification of temperature changes has been inferred in the Caribbean during Heinrich Stadial 114, it is also possible that some of the observed increase in OS δ^{18} O values during H1 is related to cooling.

Hydroclimate variability during the Bølling-Allerød (B/A)

To understand Caribbean regional dynamics' impact on our speleothem record, we compared it with the sediment reflectance record from the Cariaco Basin, a key indicator of tropical hydrological variability linked with high-latitude climate events^{19,70} (Fig. 5). Reflectance is a proxy for changes in sediment composition and highlights variability in the relative contributions of terrigenous and biogenic components, which depends on rain amounts¹⁹. Prior to ~15.5 kyrs BP, the OS and Cariaco Basin records align with highlatitude millennial climate events (Fig. 6A) and are consistent with each other. Both show a decline of rainfall until ~16.5 kyrs, following by the most arid conditions of this interval and increased variability. However, after ~15.5 kyrs BP, their similarity diminishes, evident from diverging patterns in both records; for instance, the Cariaco Basin record has a gradual trend towards wetter conditions between ~15.5 and 14.7 kyrs BP, whereas the OS δ^{18} O record does not, portraying instead multiple dry episodes during this window (Fig. 5). During the B/A time interval (after 14.6 kyrs BP), however, both records show a significant trend indicative of a transition to wetter climate conditions across the Caribbean, distinct from H1 conditions, coinciding with AMOC strengthening and North Atlantic warming (Figs. 4-5, S3).

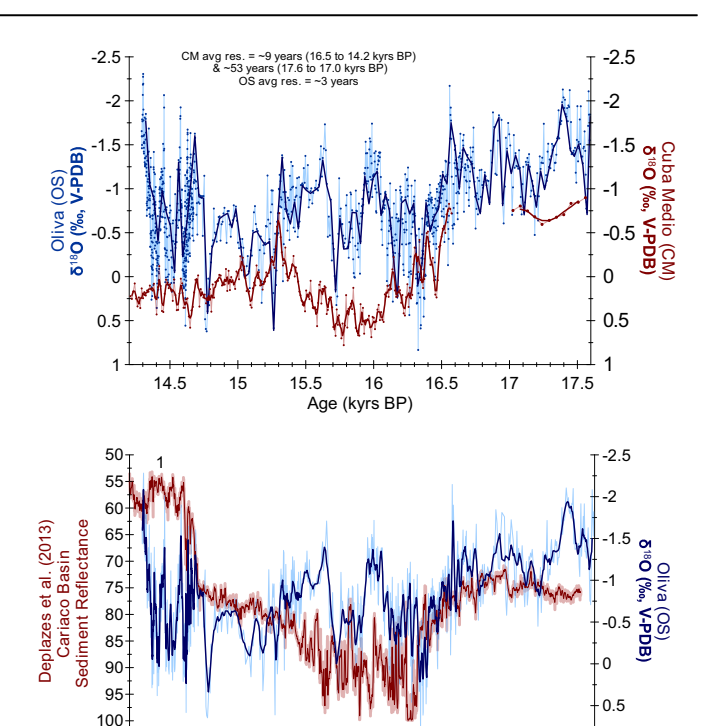


Fig. 5 | Top panel: OS δ^{18} O record (blue) plotted with CM δ^{18} O record²² (red). Lighter blue and red lines represent the OS and CM δ^{18} O data (respectively), and the darker lines in front are the running averages with matched resolution of ~50 years. Little replication between the two is observed, with a ~ 2 times larger δ^{18} O amplitude in OS (0.8 to -2.4%) than in CM (0.8 to -0.9%). Lower panel: OS δ^{18} O record (blue) plotted with the Cariaco Basin sediment reflectance record (red¹⁹;) over the entire OS record. Downward on the y-axes indicates drier conditions. The Bølling–Allerød (B/A) warm interval is marked as "1". Reflectance is a proxy for changes in sediment composition and highlights variability in the relative contributions of terrigenous and biogenic components, which depend on rain amounts¹⁹.

16

105

15

Given the northern position of Cuba and that the Gulf of Mexico serves as one of the primary moisture sources to the region 71,72 , we also consider the potential impact of freshwater forcing to the Gulf of Mexico during the last deglaciation. Multiple pulses of meltwater input via the Mississippi River to the Gulf of Mexico have been suggested, one between $\sim\!16.4$ and 15.7 kyrs BP and a second between $\sim\!15.2$ and 13.1 kyrs BP (peaking during the B/A) from the Orca Basin, 300 km south of the Mississippi River (Core MD02-2550) 73,74 . These meltwater pulses may have driven a portion of the observed discrepancies between regional records. For example, it is possible that some of the divergence between the OS δ^{18} O and Cariaco Basin records could be explained by this, such as between $\sim\!15.5$ and 14.7 kyrs BP when Cariaco is getting wetter while western Cuba experiences several dry episodes. Locations such as Cariaco Basin or Lake Petén Itzá, which are located further south, would likely see less hydroclimate impacts from Gulf of Mexico meltwater inputs.

Interestingly, the trend from H1 to B/A in the OS isotopic record and growth rates contrasts with the CM stalagmite $\delta^{18}O$ record from the same period where no transition is apparent (Fig. 5). This discrepancy suggests that the OS record is more in line during this time with records from the Gulf of Mexico²¹, Bahamas⁵¹, and the Cariaco Basin¹⁵, reflecting a distinct regional response to the transition from H1 to the B/A (Figs. 5–6). As another line of evidence, the OS $\delta^{234}U_{initial}$ values (Fig. S8) during this transition support a similar rapid response, with distinctively lower values during the B/A (Fig. S8), consistent with our hydroclimate interpretation from the OS growth rate and stable isotope records.

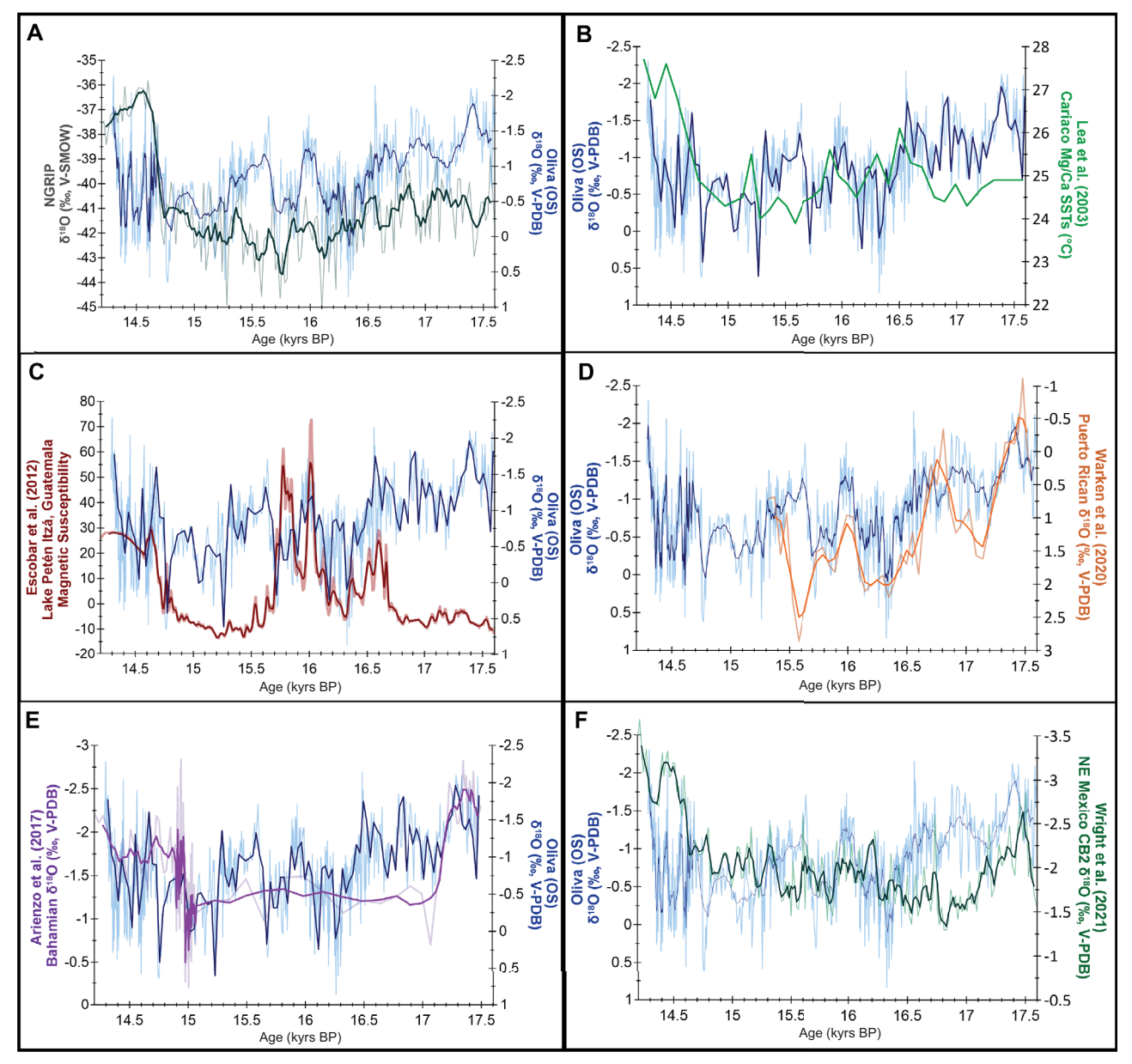


Fig. 6 | OS δ^{18} O record (blue) plotted with various records from the Caribbean region and other relevant records. These include A NGRIP¹¹², B Cariaco Basin Core PL07-39PC Mg/Ca SST record⁷⁰, C Lake Peten Itza magnetic susceptibility record¹², D PR-LA-1 speleothem record from Puerto Rico²⁴, E AB-DC-09

speleothem record from the Bahamas $^{\rm 51}$, and F CB2 speleothem record from NE Mexico $^{\rm 21}$. Lighter lines represent the original data from the records, and the darker lines in front are the running averages with matched resolutions to the record being compared to.

Modeling studies and paleoclimate research indicate significant warming in the tropical North Atlantic during the B/A, accompanied by a northward shift in the ITCZ's mean position \$\(^{8,15,19,70,75,76}\). Speleothem growth rates during H1 were consistently low, divided into two phases. However, during the B/A, we observed two significant surges in growth rates, indicating increased rainfall, interspersed with drier periods reaching, briefly, near H1 conditions. The ITCZ, as noted in earlier studies, typically does not extend to the latitudes of Cuba, and these shifts were likely less than 1° latitude 25,26. The warming of the North Atlantic likely intensified convection in the region, thereby strengthening the regional Hadley circulation. This process could have enhanced the North Atlantic Subtropical High (NASH), potentially also affecting its geographical position.

Modeling studies support this hypothesis, suggesting that a warming North Atlantic, similar to trends observed in anthropogenic global warming, results in a more intense NASH that tends to shift westward from its usual location 77.78. This westward displacement of the NASH on seasonal

timescales significantly influences rainfall patterns, particularly in the southeastern United States and the northern Caribbean, increasing climatic variability and leading to alternating periods of enhanced rainfall interrupted by declines 77.78. The Atlantic Warm Pool (AWP) is another important modifier of the extent of moisture provided to the region; it appears in the Caribbean in summer, then expands into the Gulf of Mexico, weakening NASH and enhancing rainfall when temperatures rise 14.79. On this note, it has been suggested that late glacial to early Holocene rainfall in this region was linked to the AWP through a threshold for tropical convection (~26 °C), wherein below this threshold aridity abruptly increased due to atmospheric stability, while during warm intervals like the B/A and Holocene, the SST convection threshold was surpassed, resulting in increased rainfall and instability 14.

Finally, we would like to point out that our paleoclimate record from Cuba, indicating significant rainfall fluctuations during the last deglaciation, reflects the inherent variability in hydroclimate regardless of the overall

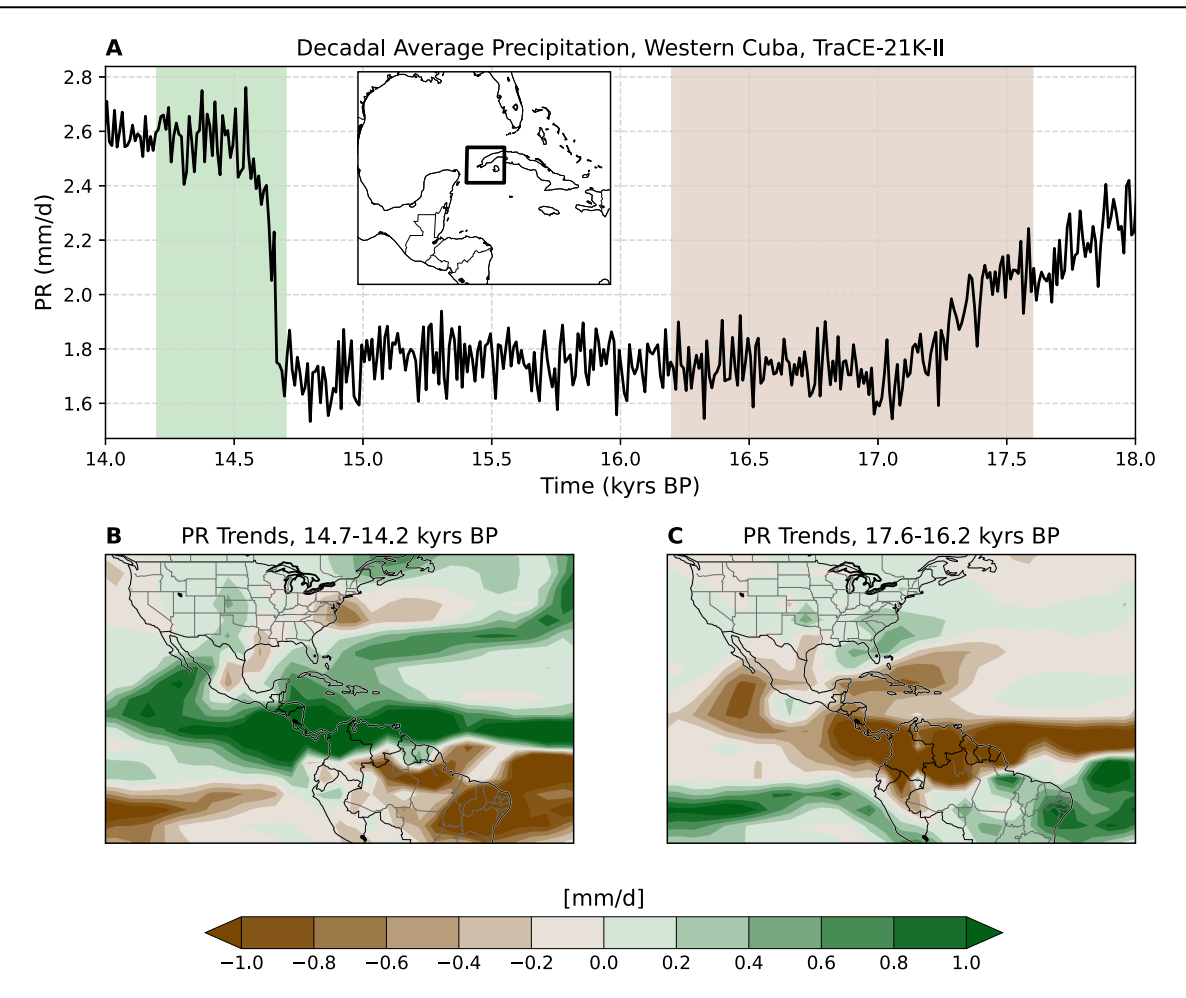


Fig. 7 | Simulated rain amounts in western Cuba. A During the interval of interest covered by our record from TraCE-21K-II, the CCSM3-based transient all-forcing paleoclimate simulation⁸⁴. The model supports the overall millennial-scale

variations seen in our record. The highlighted green and brown boxes (\mathbf{A}) are shown in (\mathbf{B} , \mathbf{C}), respectively, as regional rainfall trends during the (\mathbf{B}) B/A and (\mathbf{C}) early deglaciation periods.

climate state. This observation is consistent with numerous speleothem records across the tropical Americas. During the B/A, wet and dry conditions were not persistent but interspersed with intermittent opposite phases. Multiple paleoclimate studies e.g. ^{21,51,69,80}, from both hemispheres show this (illustrated in Figs. S5, S6; see Supplementary Information). This pattern of fluctuating hydroclimate is further supported by contemporary instrumental records, highlighting a common occurrence of high rainfall variability in the region across various timescales—seasonal, annual, and interannual^{71,81–83}. These findings highlight the complex and dynamic nature of tropical hydroclimate systems, particularly in the context of significant climatic events like the last deglaciation.

Drivers of rain amounts in Cuba on millennial timescales

The factors influencing Cuban (and more generally Caribbean) rainfall over millennial timescales are complex and multifaceted. A significant factor is the variability in SSTs within the tropical-subtropical North Atlantic and Caribbean regions. This is evidenced by the relationship between the OS stalagmite $\delta^{18}O$ record and the Mg/Ca SST record from Core PL07-39PC in the western tropical Atlantic, specifically in the Cariaco Basin (Fig. 6B). Warmer SSTs in the Mg/Ca record are associated with increased rainfall and lower OS $\delta^{18}O$ values (and vice versa). Our research suggests that the mean position of the ITCZ alone is not the primary determinant of regional hydroclimate. This is evident from several lines of evidence: (1) the Cariaco Basin record diverging from the OS record between ~15.5 and 14.7 kyrs BP, suggesting hydroclimate influences beyond the ITCZ shift (Fig. 5); (2) the significant correlation between OS $\delta^{18}O$ values and SSTs from the western tropical Atlantic, reinforcing the role of SST-driven changes in regional

convection (Fig. 6B)⁷⁰; (3) the influence of AMV and ENSO on hydroclimate variability as revealed by wavelet analysis (Fig. 4)^{41–44,46}; and (4) proxy-model comparisons (TraCE-21K-II) that capture millennial-scale hydroclimate variability consistent with OS records and North Atlantic climate shifts (Fig. 7A)⁸⁴. These findings highlight the role of dynamic ocean-atmosphere interactions beyond simple ITCZ migration in modulating rainfall patterns.

During events such as H1, cooling of the northern tropics likely resulted in reduced convection within the ITCZ, subsequently decreasing the moisture available to regional weather systems like the CLLJ. This mechanism also affects broader Atlantic tropical cyclone activity, potentially influencing their frequency and intensity. Our findings thus move beyond focusing solely on the position of the ITCZ, highlighting the importance of SSTs per se and SST-induced changes in the intensity of regional convection as key factors in Caribbean hydroclimate variability. Recent modeling and paleoclimate studies^{21,37,38,85} reinforce the significant influence of SST variability on historical rainfall patterns in the Caribbean and Gulf of Mexico. Furthermore, the behavior of the NASH and the AWP, as discussed earlier 77,78, introduces an additional layer to these intricate interactions, emphasizing the complexity of understanding rainfall drivers in the Caribbean over millennial timescales. These results highlight that while ITCZ migration plays a role in regional hydroclimate shifts, multiple interacting factors, including SST-driven convection, AMOC variability, NASH displacement, and internal variability from AMV and ENSO, contribute to the observed hydroclimate responses. This complexity underscores the need for an integrative approach to interpreting past rainfall patterns, considering both atmospheric and oceanic influences.

Proxy-model comparison and directions for future research

To investigate if we can provide a model-based justification for the hydroclimate changes observed in the OS stalagmite proxy results, we analyzed rainfall amounts simulated by the CCSM3-based all-forcing paleoclimate model experiment called the Simulation of Transient Climate Evolution over the last 21,000 years (TraCE-21K-II)^{8,84}. The preliminary analysis of simulated rainfall over western Cuba in the TraCE-21K-II model shows that the millennial-scale rainfall variability aligns well with the hydroclimate shifts observed in the OS stalagmite record (Fig. 7A). Notably, the simulated trends during the B/A and early deglaciation (Fig. 7B, C) correspond with the transition from drier H1 conditions to wetter B/A conditions, supporting the role of SST-driven convection changes rather than a simple ITCZ latitudinal shift. Additional model-based analyses could further elucidate the mechanistic links between SST variability, atmospheric circulation, and rainfall in the northern Caribbean.

These spatial trends shown in Fig. 7B, C agree with previous observations of an out of phase hydroclimate response across the equator on millennial timescales, aligning regional climatic shifts in the Caribbean supported by our OS results with these significant high-latitude events. The encouraging proxy-model comparison deserves further examination, as the model-based analyses may be used to explore the proposed underlying mechanisms related to atmospheric and SST variability and support inferences drawn from proxy records.

Conclusions

The OS speleothem growth rates and proxy records (δ^{13} C, δ^{18} O, and δ^{234} Uinitial values) from our study demonstrate significant hydroclimate variability during Heinrich event 1 (H1) and the Bølling-Allerød (B/A) period, showing trends that are consistent with other Caribbean and Gulf of Mexico records. During H1, particularly H1.1 (16.2 kyrs BP) and H1.2 (15.1 kyrs BP), the OS record indicates peak aridity in western Cuba, as evidenced by high stalagmite δ^{18} O values, aligning with the weakest phases of the Atlantic Meridional Overturning Circulation (AMOC). This pattern corresponds with more humid conditions indicated by lower stalagmite δ^{18} O values before 16.4 kyrs BP, when AMOC was stronger and North Atlantic SSTs were higher.

In the transition to the B/A period, after 14.7 kyrs BP, the OS records, alongside the Cariaco Basin, Bahamas, and Gulf of Mexico records, show a shift towards wetter conditions, differing from those in H1. This is further evidenced by significant surges in OS growth rates, indicating increased rain amounts interspersed with drier periods. These records provide a precise chronology, aligning regional climatic shifts in the Caribbean with these significant high-latitude events, in agreement with previous observations of an out-of-phase hydroclimate response across the equator on millennial timescales. However, our findings reveal that hydroclimate variability is not solely dictated by large-scale hemispheric shifts but is influenced by multiple, interacting processes operating across different timescales. These include internal climate variability (AMV, ENSO), regional atmospheric circulation changes, and tropical cyclone dynamics, which imprint strong interannual to decadal variability on longer-term climatic trends.

Lastly, our study underscores the multi-factorial nature of hydroclimate drivers in Cuba and the broader Caribbean, emphasizing the interplay of oceanic and atmospheric mechanisms beyond ITCZ migration alone. Central to this is the variability of SSTs in the tropical-subtropical North Atlantic and Caribbean, which significantly modulates regional hydroclimate through its influence on convective intensity, atmospheric moisture availability, and tropical cyclogenesis. Additionally, the position and intensity of the North Atlantic Subtropical High (NASH) respond to SST variations, further shaping rainfall patterns through changes in wind patterns and moisture transport. These insights highlight the dynamic nature of hydroclimate in the region, where rainfall patterns are not static but rather evolve in response to shifting oceanic and atmospheric conditions.

The encouraging proxy-model comparison with TraCE-21K-II supports these interpretations, reinforcing the role of SST-driven convection in

hydroclimate variability and providing an avenue for further investigations into the underlying mechanisms. Future research should focus on refining the proxy-model relationship, particularly in capturing high-frequency climate variability and better resolving the specific contributions of AMOC, AMV, and NASH variability to past rainfall trends in the Caribbean.

Methods

Cave and collection site

The OS stalagmite was retrieved from the chamber locally known as *Salón de la Permanencia Subterránea* (SPS), located within the Upper Cave of the Majaguas Stream in the *Majaguas-Cantera cave system* (MCCS) (Fig. 1). This extensive 35-km cave system located in the western Cuban province of Pinar del Rio (22°23′N; 83°58′W) is situated in the karst region of *Sierra de San Carlos*, part of the *Sierra de los Órganos* mountain range. The MCCS comprises nine underground levels with elevations ranging from 50 to 290 m³6. In the hydrological years of 2008-2009, partial cave monitoring took place in the MCCS, particularly in Dos Anas cave. Dos Anas cave shares similar environmental characteristics with SPS and is located nearby, approximately 2 km from the OS collection point⁵3. Monitoring data indicated that the cave's air temperature fluctuated between 21.3 °C to 21.5 °C, while relative humidity consistently maintained levels near 100% throughout the year.

Stable isotope composition and U/Th dating

The OS stalagmite δ^{18} O and δ^{13} C compositions were determined in the Stable Isotope Laboratory at the University of Massachusetts Amherst, using an on-line carbonate preparation system linked to a Thermo Scientific Delta Plus isotope ratio mass spectrometer. Reproducibility of the standard material is better than $\pm 0.1\%$. All values are reported relative to the V-PDB standard⁸⁷. The OS chronology was built using the U-series dating technique⁸⁸. Calcite powder samples, each weighing around 0.3 g, were collected from the speleothem using a micromill. After collection, U/Th analyses were performed using a multi-collector inductively coupled plasma mass spectrometer (MC-ICP-MS) in the Paleoclimate and Geochronology Laboratory at the Massachusetts Institute of Technology (MIT). Before measurement, samples were dissolved, spiked, and uranium and thorium were separated following standard techniques⁸⁸. The OS age model was developed using the COPRA software⁸⁹ using default interpolation with 2000 Monte Carlo simulations in MatLab.

Isotopic equilibrium conditions

Speleothems provide information on past climate variability; however, the δ^{13} C and δ^{18} O signals in a speleothem depend in part on processes occurring inside the cave. Under certain conditions $\delta^{13}C$ and $\delta^{18}O$ values can be driven out of isotopic equilibrium with the drip water, resulting in a speleothem isotope signal that does not reflect the isotopic value of the drip water and impacting the reliability of hydroclimate interpretations above the cave⁶⁷. Empirical isotopic equilibrium calculations carried out on another speleothem from Dos Anas cave, stalagmite CG, support the notion that speleothem calcite formation occurs under or near isotopic equilibrium conditions, which may suggest similar conditions for stalagmites OS^{37,38,53,90}. While monitoring data is not available from the SPS, its proximity to the Majaguas stream likely contributes to consistently high humidity levels, maintaining them at nearly 100% throughout the year, analogous to Dos Anas cave. It is noteworthy that the complex karst landscape in Sierra de San Carlos, coupled with neotectonics in the region, has had a significant impact on lithological and structural rock conditions, including the potential opening and blocking of infiltration pathways for speleothems⁸⁶. In order to investigate whether stalagmite OS was formed under isotopic equilibrium conditions, we performed calculations of calcite isotopic composition expected from given environmental conditions using the equation from ref. 67. These calculations consider observed yearly cave air temperature for the MCCS (21.5 °C), estimated atmospheric surface temperature changes in the northern Caribbean during the deglacial period⁹¹, and the range of annual δ^{18} O composition of rainfall in western Cuba based on instrumental data from the IAEA-GNIP database (-1.0% to -4.0%) (Fig. 2).

Given the physicochemical attributes of the MCCS, including high relative humidity 37,38,53 , and isotopic equilibrium insights from our calculations of calcite $\delta^{18}O$ composition (see Table S1), we infer that the OS stalagmite likely formed under conditions close to isotopic equilibrium with its drip water. This positions the OS stalagmite as a valuable recorder of past rainfall patterns. This working hypothesis is bolstered by related studies in the same cave $^{37-39,52}$. It is also key to note that a relationship between $\delta^{13}C$ and $\delta^{18}O$ does not necessarily imply disequilibrium. Despite one of the outdated Hendy criteria stipulating that there is no relationship between $\delta^{13}C$ and $\delta^{18}O$ when calcite is deposited at equilibrium conditions 90 , this can only be true if $\delta^{13}C$ is not influenced by climate 92 . In this case and many others, particularly in the tropics, the primary determinator of both $\delta^{13}C$ and $\delta^{18}O$ is rainfall, and thus one would expect a coupling of the records.

Regional climate and climate drivers

Pinar del Rio Province experiences tropical climate characterized by distinct dry and rainy seasons. The dry season typically extends from November to April, while the rainy season spans from May to October^{81,93}. The annual average temperature in the area is 24.9 °C, and it receives an average of 1700 mm/year of rainfall⁹⁴. The North Atlantic Subtropical High (NASH) briefly intensifies in midsummer, leading to a midsummer drought and resulting in a slightly bimodal rainfall pattern^{71,72,81,82,93}.

The Caribbean, Gulf of Mexico, and tropical North Atlantic serve as the primary moisture sources to the region^{71,72}. Seasonal rainfall variability in Cuba is influenced by several interrelated factors, including the Caribbean Low-Level Jet (CLLJ), the NASH, Caribbean and tropical Atlantic sea surface temperatures (SSTs), easterly waves, the eastern tropical Pacific, and indirectly, the movement of the ITCZ (related to the influence on NASH and the CLLJ)^{72,95–97}. Climate anomalies on sub-decadal to multidecadal timescales in the wider Caribbean region are influenced by the North Atlantic Oscillation (NAO), the Atlantic Multidecadal Variability (AMV), and the El Niño Southern Oscillation (ENSO)^{58,62,72,98}.

The 'amount effect' relationship and its implications

The presence of an 'amount effect' relationship, linking rainfall amount to its δ^{18} O composition, has been widely observed in tropical regions, including the Caribbean e.g. refs. 23,29,30,38,99. This relationship is corroborated by IAEA-GNIP data from Havana, Cuba (Fig. 2). Medina-Elizalde et al. $(2017)^{23}$ observed a consistent relationship which quantitatively defines the 'amount effect' across the Gulf of Mexico and Caribbean based on instrumental isotopic data. Furthermore, evidence of a seasonal amount effect extends north of the Gulf of Mexico into the southeastern United States¹⁰⁰.

The enduring stability of the amount effect across diverse geographic regions supports its presence in Cuba across various climate states, including glacial-interglacial periods. However, it is important to consider changing conditions during the deglacial period, which may have shifted rainfall $\delta^{18}O$ values. During the last glacial period, the extensive continental ice sheets resulted in the ocean's $\delta^{18}O$ composition ($\delta^{18}O$ sw) being ~1.2% higher than current levels. Additionally, model experiments suggest that the $\delta^{18}O$ of rainfall in the North Atlantic during this period could have been 1.6% more positive compared to modern times 101,102 . This effect lessened during the deglaciation, as seen in the $\delta^{18}O$ sw Caribbean record 103 , indicating an overall ~0.4% decrease during the period covered by the OS isotopic records. Although we have accounted for this change in our equilibrium calculations for the OS stalagmite (Table S1), we acknowledge the uncertainty in our estimates propagating from the unconstrained oxygen isotope composition of the ocean through the period of interest.

Statistical data analysis

Wavelet spectral analysis, cross-correlation, and wavelet correlation analysis were performed using the R package biwavelet (version 0.20.19 and available freely from https://cran.r-project.org/package=biwavelet¹⁰⁴⁻¹⁰⁶). Unevenly

spaced time series of δ^{18} O and δ^{13} C were interpolated to the mean resolution of one year by the Akima splines method ¹⁰⁷, one of the most common, useful, and effective methods to interpolate unevenly spaced paleoclimate time series ^{108,109}. In addition, we have corroborated whether this interpolation method works properly with our data by comparing the interpolated time series with the original unevenly spaced one and found differences to be negligible. We have used the R package Pracma (version 2.3.3, available freely from https://CRAN.R-project.org/package=pracma¹¹⁰) that includes the Akima method to interpolate the δ^{18} O and δ^{13} C time series.

Data availability

The OS oxygen and carbon isotope data presented in this paper are available online on the NOAA Paleoclimatology database (https://www.ncei.noaa.gov/access/paleo-search/study/41960).

Received: 10 July 2024; Accepted: 10 June 2025; Published online: 01 July 2025

References

- Morgan, V. et al. Relative timing of deglacial climate events in Antarctica and Greenland. Science 297, 1862–1865 (2002).
- Clark, P. U. et al. Global climate evolution during the last deglaciation. *Proc. Natl. Acad. Sci. USA* 109, E1134–E1142 (2012).
- Bahr, A. et al. Low-latitude expressions of high-latitude forcing during Heinrich Stadial 1 and the Younger Dryas in northern South America. Glob. Planet. Change 160, 1–9 (2018).
- 4. Hodell, D. A. et al. Anatomy of Heinrich Layer 1 and its role in the last deglaciation. *Paleoceanography* **32**, 284–303 (2017).
- Naafs, B. D. A., Hefter, J., Grützner, J. & Stein, R. Warming of surface waters in the mid-latitude North Atlantic during Heinrich events. *Paleoceanography* 28, 153–163 (2013).
- Martrat, B., Jimenez-Amat, P., Zahn, R. & Grimalt, J. O. Similarities and dissimilarities between the last two deglaciations and interglaciations in the North Atlantic region. *Quat. Sci. Rev.* 99, 122–134 (2014).
- Heinrich, H. Origin and consequences of cyclic ice rafting in the northeast Atlantic Ocean during the past 130,000 years. *Quat. Res.* 29, 142–152 (1988).
- Liu, Z. et al. Transient simulation of last deglaciation with a new mechanism for Bølling-Allerød warming. Science 325, 310–314 (2009).
- Stocker, T. F. & Johnsen, S. J. A minimum thermodynamic model for the bipolar seesaw. *Paleoceanography* 18, 1–11 (2003).
- Broecker, W. S. Paleocean circulation during the last deglaciation: a bipolar seesaw?. *Paleoceanography* 13, 119–121 (1998).
- Peterson, L. C., Haug, G. H. & Hughen, K. A. & Röhl, U. Rapid changes in the hydrologic cycle of the tropical atlantic during the last glacial. Science 290, 1947–1951 (2000).
- Escobar, J. et al. A similar to 43-ka record of paleoenvironmental change in the Central American lowlands inferred from stable isotopes of lacustrine ostracods. *Quat. Sci. Rev.* 37, 92–104 (2012).
- Hodell, D. A. et al. An 85-ka record of climate change in lowland Central America. Quat. Sci. Rev. 27, 1152–1165 (2008).
- Hodell, D. A. et al. Late Glacial temperature and precipitation changes in the lowland Neotropics by tandem measurement of delta O-18 in biogenic carbonate and gypsum hydration water. Geochim. Cosmochim. Acta 77, 352–368 (2012).
- Wang, Y. J. et al. A high-resolution absolute-dated Late Pleistocene monsoon record from Hulu Cave, China. Science 294, 2345–2348 (2001).
- Wang, X. et al. Millennial-scale precipitation changes in southern Brazil over the past 90,000 years. *Geophys. Res. Lett.* 34, L23701 (2007).

- Bradley, R. S. & Diaz, H. F. Late quaternary abrupt climate change in the tropics and sub-tropics: the continental signal of tropical hydroclimatic events (THEs). Rev. Geophys. 59, 1–35 (2021).
- Ramirez, V. M. et al. Summer insolation controlled movements of Intertropical Convergence Zone during last glacial cycle in northern South America. Commun. Earth Environ. 4, 495 (2023).
- Deplazes, G. et al. Links between tropical rainfall and North Atlantic climate during the last glacial period. Nat. Geosci. 6, 213–217 (2013).
- Wang, X. et al. Wet periods in northeastern Brazil over the past 210 kyr linked to distant climate anomalies. *Nature* 432, 740–743 (2004).
- Wright, K. T. et al. Thermodynamics control precipitation in NE Mexico on orbital to millennial timescales. *Nat. Commun.* 1-24, https://doi.org/10.21203/rs.3.rs-611282/v1 (2021).
- Warken, S. F. et al. Caribbean hydroclimate and vegetation history across the last glacial period. Quat. Sci. Rev. 218, 75–90 (2019).
- Medina-Elizalde, M. et al. Synchronous precipitation reduction in the American Tropics associated with Heinrich 2. Sci. Rep. 7, 11216 (2017).
- Warken, S. F. et al. Persistent link between Caribbean precipitation and Atlantic Ocean circulation during the Last Glacial revealed by a speleothem record from Puerto Rico. *Paleoceanogr. Paleoclimatol.* 35, 1–17 (2020).
- McGee, D., Donohoe, A., Marshall, J. & Ferreira, D. Changes in ITCZ location and cross-equatorial heat transport at the Last Glacial Maximum, Heinrich Stadial 1, and the mid-Holocene. *Earth Planet*. *Sci. Lett.* 390, 69–79 (2014).
- Donohoe, A., Marshall, J., Ferreira, D. & McGee, D. The relationship between ITCZ location and cross-cquatorial atmospheric heat transport: from the seasonal cycle to the Last Glacial Maximum. *J. Clim.* 26, 3597–3618 (2013).
- Asmerom, Y. et al. Intertropical convergence zone variability in the Neotropics during the Common Era. Sci. Adv. 6, 1 (2020).
- Ridley, H. et al. Aerosol forcing of the position of the intertropical convergence zone since AD 1550. *Nat. Geosci.* 8, https://doi.org/10. 1038/ngeo2353 (2015).
- Dansgaard, W. Stable Isotopes in Precipitation. *Tellus* 16, 436–468 (1964).
- Vuille, M. et al. Modeling delta O-18 in precipitation over the tropical Americas: 2. Simulation of the stable isotope signal in Andean ice cores. J. Geophys. Res. Atmos. 108 (2003).
- Medina-Elizalde, M. et al. High-resolution speleothem record of precipitation from the Yucatan Peninsula spanning the Maya Preclassic Period. Glob. Planet. Change 138, 93–102 (2016).
- Lachniet, M. S. & Patterson, W. P. Oxygen isotope values of precipitation and surface waters in northern Central America (Belize and Guatemala) are dominated by temperature and amount effects. *Earth Planet. Sci. Lett.* 284, 435–446 (2009).
- Lachniet, M. S. Climatic and environmental controls on speleothem oxygen-isotope values. Quat. Sci. Rev. 28, 412–432 (2009).
- Medina-Elizalde, M. et al. High resolution stalagmite climate record from the Yucatan Peninsula spanning the Maya terminal classic period. Earth Planet. Sci. Lett. 298, 255–262 (2010).
- 35. Fairchild, J. & Baker, A. Speleothem Science: from Process to Past Environments. (Wiley-Blackwell, 2012).
- Serrato et al. Evidence for decreased precipitation variability in the Yucatán Peninsula during the mid-holocene. *Paleoceanogr. Paleoclimatol.* 36, 1–21 (2021).
- Fensterer, C. et al. Cuban stalagmite suggests relationship between Caribbean precipitation and the Atlantic Multidecadal Oscillation during the past 1.3 ka. Holocene 22, 1405–1412 (2012).
- Fensterer, C. Holocene Caribbean Climate Variability Reconstructed from Speleothems from Western Cuba. (Ruperto-Carola University of Heidelberg, 2011).

- 39. Fensterer, C. et al. Millennial-scale climate variability during the last 12.5 ka recorded in a Caribbean speleothem. *Earth Planet. Sci. Lett.* **361**, 143–151 (2013).
- Hatvani, I. G. et al. The SISAL webApp: exploring the speleothem climate and environmental archives of the world. *Quat. Res.* 1-7 (2023).
- Moura, A. D. & Shukla, J. On the dynamics of droughts in northeast Brazil: Observations, theory and numerical experiments with a general circulation model. *J. Atmos. Sci.* 38, 2653–2675 (1981).
- Knight, J. R., Folland, C. K. & Scaife, A. A. Climate impacts of the atlantic multidecadal oscillation. *Geophys. Res. Lett.* 33, L17706 (2006).
- Medina-Elizalde, M., Polanco-Martinez, J. M., Lases-Hernandez, F., Bradley, R. & Burns, S. Testing the "tropical storm" hypothesis of Yucatan Peninsula climate variability during the Maya terminal classic period. Quat. Res. 86, 111–119 (2016).
- Wang, C. & Lee, S. K. Global warming and United States landfalling hurricanes. Geophys. Res. Lett. 35, 1–4 (2008).
- Wang, C., Lee, S.-K. & Enfield, D. B. Climate response to anomalously large and small atlantic warm pools during the summer. J. Clim. 21, 2437–2450 (2008).
- Kossin, J. P. A global slowdown of tropical-cyclone translation speed. *Nature* 558, 104–107 (2018).
- Broecker, W. & Putnam, A. E. How did the hydrologic cycle respond to the two-phase mystery interval?. Quat. Sci. Rev. 57, 17–25 (2012).
- 48. Broecker, W. The mysterious 14C decline. *Radiocarbon* **51**, 109–119 (2009).
- Zhang, W. et al. A detailed East Asian monsoon history surrounding the 'Mystery Interval' derived from three Chinese speleothem records. Quat. Res. 82, 154–163 (2014).
- McManus, J. F., Francois, R., Gherardi, J.-M., Keigwin, L. D. & Brown-Leger, S. Collapse and rapid resumption of Atlantic meridional circulation linked to deglacial climate changes. *Nature* 428, 834–837 (2004).
- Arienzo, M. M. et al. Multi-proxy evidence of millennial climate variability from multiple Bahamian speleothems. *Quat. Sci. Rev.* 161, 18–29 (2017).
- Brahim, Y. A. et al. Hydroclimate variability in the Caribbean during North Atlantic Heinrich cooling events (H8 and H9). Sci. Rep. 12, 1–12 (2022).
- Pajón, J. M. et al. Monitoreo quimico-fisico e isotopico de las aguas de flujo hipodermico de la cueva Dos Anas (Sierra de San Carlos) y la cueva Antorcha (Sierra de Quemados), Sierra de los Organos, Pinar del Rio, Cuba., 45 (Germany, 2009).
- 54. Ford, D. & Williams, P. D. Karst hydrogeology and geomorphology. (John Wiley & Sons, 2013).
- Hellstrom, J. C. & McCulloch, M. T. Multi-proxy constraints on the climatic signicance of trace element records from a New Zealand speleothem. Earth Planet. Sci. Lett. 179, 287–297 (2000).
- Patterson, E. W. et al. Glacial changes in sea level modulated millennial-scale variability of Southeast Asian autumn monsoon rainfall. PNAS 120, 1–8 (2023).
- Gray, S. T., Graumlich, L. J., Betancourt, J. L. & Pederson, G. T. A tree-ring based reconstruction of the Atlantic multidecadal oscillation since 1567 A.D. *Geophys. Res. Lett.* 31, L12205 (2004).
- Bhattacharya, T., Chiang, J. C. H. & Cheng, W. Ocean-atmosphere dynamics linked to 800-1050 CE drying in mesoamerica. *Quat. Sci. Rev.* 169, 263–277 (2017).
- Enfield, D. B., Mestas-Nuñez, A. M. & Trimble, P. J. The Atlantic multidecadal oscillation and its relation to rainfall and river flows in the continental US. *Geophys. Res. Lett.* 28, 2077–2080 (2001).
- Winter, A. et al. Evidence for 800years of North Atlantic multidecadal variability from a Puerto Rican speleothem. *Earth Planet.* Sci. Lett. 308, 23–28 (2011).

- Jury, M. R. Inter-annual rainfall variability in the eastern Antilles and coupling with the regional and intra-seasonal circulation. *Theor.* Appl. Climatol. 126, 727–737 (2016).
- 62. Chen, A. A. & Taylor, M. A. Investigating the link between early season Caribbean rainfall and the El Niño + 1 year. *Int. J. Climatol.* **22**, 87–106 (2002).
- Goldenberg, S. B. & Shapiro, L. J. Physical mechanisms for the Association of El Niño and West African rainfall with Atlantic Major Hurricane Activity. J. Clim. 9, 1169–1187 (1996).
- Patricola, C. M., Saravanan, R. & Chang, P. The impact of the El Niño-Southern Oscillation and Atlantic meridional mode on seasonal Atlantic tropical cyclone activity. *J. Clim.* 27, 5311–5328 (2014).
- Tang, B. H. & Neelin, J. ENSO influence on Atlantic hurricanes via tropospheric warming. *Geophys. Res. Lett.* 31, 1–4 (2004).
- Warken, S. F. et al. Solar forcing of early Holocene droughts on the Yucatán peninsula. Sci. Rep. 11, 1–12 (2021).
- Hansen, M., Scholz, D., Schöne, B. R. & Spötl, C. Simulating speleothem growth in the laboratory: determination of the stable isotope fractionation (δ13C and δ18O) between H2O, DIC and CaCO3. Chem. Geol. 509, 20–44 (2019).
- Arienzo, M. M. et al. Bahamian speleothem reveals temperature decrease associated with Heinrich stadials. *Earth Planet. Sci. Lett.* 430, 377–386 (2015).
- Stríkis, N. M. et al. Timing and structure of Mega-SACZ events during Heinrich Stadial 1. Geophys. Res. Lett. 42, 5477–5484 (2015).
- Lea, D. W., Pak, D. K., Peterson, L. C. & Hughen, K. A. Synchroneity of Tropical and High-Latitude Atlantic temperatures over the last glacial termination. *Science* 301, 1361–1364 (2003).
- Karmalkar, A. V., Bradley, R. S. & Diaz, H. F. Climate change in Central America and México: regional climate model validation and climate change projections. Clim. Dyn. 37, 605–629 (2011).
- Mestas-Nuñez, A. M., Enfield, D. B. & Zhang, C. Water vapor fluxes over the Intra-Americas Sea: Seasonal and interannual variability and associations with rainfall. J. Clim. 20, 1910–1922 (2007).
- Flower, B. P., Hastings, D. W., Hill, H. W. & Quinn, T. M. Phasing of deglacial warming and Laurentide Ice Sheet meltwater in the Gulf of Mexico. *Geology* 32, 597–600 (2004).
- 74. Williams, C. C. Meltwater and Abrupt Climate Change During the Last Deglaciation: A Gulf of Mexico Perspective. (University of South Florida, 2009).
- Li, S. & Liu, W. Deciphering the migration of the intertropical convergence zone during the last deglaciation. *Geophys. Res. Lett.* 49, e2022GL098806 (2022).
- Wang, Y. et al. Millennial- and orbital-scale changes in the East Asian monsoon over the past 224,000[thinsp]years. *Nature* 451, 1090-1093, http://www.nature.com/nature/journal/v451/n7182/suppinfo/ nature06692_S1.html (2008).
- Li, W., Li, L., Fu, R., Deng, Y. & Wang, H. Changes to the North Atlantic Subtropical high and its role in the intensification of summer rainfall variability in the Southeastern United States. *J. Clim.* 24, 1499–1506 (2011).
- Luo, H., Adames, ÁF. & Rood, R. B. A northern hemispheric wave train associated with interannual variations in the Bermuda High during Boreal Summer. *J. Clim.* 34, 6163–6173 (2021).
- Martinez, C., Goddard, L., Kushnir, Y. & Ting, M. Seasonal climatology and dynamical mechanisms of rainfall in the Caribbean. Clim. Dyn. 53, 825–846 (2019).
- Novello, V. F. et al. A high-resolution history of the South American Monsoon from Last Glacial Maximum to the Holocene. Sci. Rep. 7, 1–8 (2017).
- Hastenrath, S. Interannual variability and annual cycle: mechanisms of circulation and climate in the tropical Atlantic sector. *Monthly Weather Rev.* 112, 1097–1107 (1984).

- Magaña, V., Amador, A. J. & Medina, S. The midsummer drought over Mexico and Central America. J. Clim. 12, 1577–1588 (1999).
- 83. Waliser, D. E. & Gautier, C. A Satellite-derived climatology of the ITCZ. J. Clim. 6, 2162–2174 (1993).
- 84. He, F. & Clark, P. U. Freshwater forcing of the Atlantic meridional overturning circulation revisited. *Nat. Clim. Change* **12**, 449–454 (2022).
- 85. Wright, K. T. et al. Precipitation in Northeast Mexico primarily controlled by the relative warming of Atlantic SSTs. *Geophys. Res. Lett.* **49**, 1–14 (2022).
- 86. Pajón, J. M., Hernández, I., Ortega, F. & Macle, J. *Periods of Wet Climate in Cuba: Evaluation of Expression in Karst of Sierra de San Carlos*. (Academic Press, 2001).
- 87. Sharp, Z. *Principles of Stable Isotope Geochemistry*. 344 (Pearson Prentice Hall, 2007).
- 88. Edwards, L. R., Chen, J. H. & Wasserburg, G. J. 238U234U230Th232Th systematics and the precise measurement of time over the past 500,000 years. *Earth Planet. Sci. Lett.* **81**, 175–192 (1987).
- Breitenbach, S. F. M. et al. Constructing proxy records from age models (COPRA). Climate8, 1765–1779 (2012).
- Hendy, C. H. The isotopic geochemistry of speleothems—I. The calculation of the effects of different modes of formation on the isotopic composition of speleothems and their applicability as palaeoclimatic indicators. *Geochim. Cosmochim. Acta* 35, 801–824 (1971).
- Correa-Metrio, A. et al. Rapid climate change and no-analog vegetation in lowland Central America during the last 86,000 years. Quat. Sci. Rev. 38, 63–75 (2012).
- Dorale, J. A. & Liu, Z. H. Limitations of Hendy test criteria in judging the paleoclimatic suitability of speleothems and the need for replication. *J. Cave Karst Stud.* 71, 73–80 (2009).
- Gamble, D. W., Parnell, D. B. & Curtis, S. Spatial variability of the Caribbean mid-summer drought and relation to north Atlantic high circulation. *Int. J. Climatol.* 28, 343–350 (2008).
- Díaz, C. L. R. Monografía Hidrológica de la cuenca del río
 Cuyaguateje (clima). Arch. Inst. de. Geogr.ía 191, 1–120 (1984).
- Karmalkar, A. V. et al. A review of observed and projected changes in climate for the islands in the Caribbean. *Atmósfera* 26, 283–309 (2013).
- Curtis, S. Daily precipitation distributions over the intra-Americas sea and their interannual variability. *Atmósfera* 26, 243–259 (2013).
- Magaña, V. O. & Caetano, E. in Communicating Global Change Science to Society: An Assessment and Case Studies (eds H. Tiessen, M. Brklacich, G. Breulmann, & R. S. C. Menezes) (Island Press, 2007).
- 98. Hurrell, J. W. & Deser, C. North Atlantic climate variability: the role of the North Atlantic Oscillation. *J. Mar. Syst.* **78**, 28–41 (2009).
- 99. Lases-Hernandez, F., Medina-Elizalde, M., Burns, S. & DeCesare, M. Long-term monitoring of drip water and groundwater stable isotopic variability in the Yucatán Peninsula: Implications for recharge and speleothem rainfall reconstruction. *Geochim. Cosmochim. Acta* 246, 41–59 (2019).
- Medina-Elizalde, M. et al. Southeastern United States hydroclimate during holocene abrupt climate events: evidence from new stalagmite isotopic records from Alabama. *Paleoceanogr. Paleoclimatol.* 37, 1–18 (2022).
- Caley, T., Roche, D. M., Waelbroeck, C. & Michel, E. Oxygen stable isotopes during the Last Glacial Maximum climate: perspectives from data-model (iLOVECLIM) comparison. *Climate* 10, 1939–1955 (2014).
- Risi, C., Bony, S., Vimeux, F., Jouzel, J. & Edwards, R. L. Waterstable isotopes in the LMDZ4 general circulation model: model evaluation for present-day and past climates and applications to

- climatic interpretations of tropical isotopic records. *J. Geophys. Res.* **115**, D12118 (2010).
- Schmidt, M. W., Spero, H. J. & Lea, D. W. Links between salinity variation in the Caribbean and North Atlantic thermohaline circulation. *Nature* 428, 160–163 (2004).
- Gouhier, T. C., Grinsted, A. & Simko, V. R package biwavelet: Conduct Univariate and Bivariate Wavelet Analyses (version 0.20.19). (2021).
- Liu, Y., San Liang, X. & Weisberg, R. H. Rectification of the bias in the wavelet power spectrum. *J. Atmos. Ocean. Technol.* 24, 2093–2102 (2007).
- Torrence, C. & Compo, G. P. A practical guide to wavelet analysis. Bull. Am. Meteorol. Soc. 79, 61–78 (1998).
- Akima, H. A new method of interpolation and smooth curve fitting based on local procedures. J. ACM ((JACM)) 17, 589–602 (1970).
- Schulz, M. & Stattegger, K. SPECTRUM: spectral analysis of unevenly spaced paleoclimatic time series. *Comput. Geosci.* 23, 929–945 (1997).
- Mudelsee, M. & Stattegger, K. Plio-/Pleistocene climate modeling based on oxygen isotope time series from deep-sea sediment cores: the Grassberger-Procaccia algorithm and chaotic climate systems. *Math. Geol.* 26, 799–815 (1994).
- 110. Borchers, H. W. *Pracma: Practical Numerical Math Functions*, http://CRAN.R-project.org/package=pracma (2015).
- Schneider, U. et al. Evaluating the hydrological cycle over land using the newly-corrected precipitation climatology from the Global Precipitation Climatology Centre (GPCC). Atmosphere 8, 52 (2017).
- NGRIP members High-resolution record of Northern Hemisphere climate extending into the last interglacial period. *Nature* 431, 147–151 (2004).

Acknowledgements

This work was supported by the United States National Science Foundation Grant number 2102983 (PI Medina-Elizalde). We also thank Adam Jost for his help with U/Th dating at MIT.

Author contributions

All authors contributed to this manuscript. L.T.T., M.M.E. wrote the main manuscript text and prepared the figures. M.M.E. conceptualized the project. L.T.T. produced the stable isotope data. J.M.P., M.M.E. collected the OS specimen. A.V.K. led the analyses of local climatology, TraCE-21K-II, and produced Fig. 7. J.M.P.M. carried out the wavelet spectral analyses that contributed to Figs. 4, S2, S4. L.T.T., C.W.K., D.M. conducted the U/Th

dating and prepared the chronology. D.M., A.V.K., J.M.P. contributed with evaluation of results.

Competing interests

The authors declare no competing interests.

Additional information

Supplementary information The online version contains supplementary material available at https://doi.org/10.1038/s43247-025-02465-0.

Correspondence and requests for materials should be addressed to Leah Travis-Taylor.

Peer review information Communications Earth & Environment thanks David Hodell, Yuval Burstyn, and the other anonymous reviewer(s) for their contribution to the peer review of this work. Primary Handling Editors: Ola Kwiecien, Carolina Ortiz Guerrero, Aliénor Lavergne. [A peer review file is available].

Reprints and permissions information is available at http://www.nature.com/reprints

Publisher's note Springer Nature remains neutral with regard to jurisdictional claims in published maps and institutional affiliations.

Open Access This article is licensed under a Creative Commons Attribution-NonCommercial-NoDerivatives 4.0 International License, which permits any non-commercial use, sharing, distribution and reproduction in any medium or format, as long as you give appropriate credit to the original author(s) and the source, provide a link to the Creative Commons licence, and indicate if you modified the licensed material. You do not have permission under this licence to share adapted material derived from this article or parts of it. The images or other third party material in this article are included in the article's Creative Commons licence, unless indicated otherwise in a credit line to the material. If material is not included in the article's Creative Commons licence and your intended use is not permitted by statutory regulation or exceeds the permitted use, you will need to obtain permission directly from the copyright holder. To view a copy of this licence, visit http://creativecommons.org/licenses/by-nc-nd/4.0/.

© The Author(s) 2025